CHALMERS
FINITE ELEMENT CENTER

PREPRINT 2001–22

A P^2-continuous, P^1-discontinuous finite element method for the Mindlin-Reissner plate model

Peter Hansbo and Mats G. Larson

Chalmers Finite Element Center
CHALMERS UNIVERSITY OF TECHNOLOGY
Göteborg Sweden 2001

CHALMERS FINITE ELEMENT CENTER

Preprint 2001–22

A P^2-continuous, P^1-discontinuous finite element method for the Mindlin-Reissner plate model

Peter Hansbo and Mats G. Larson

CHALMERS

Chalmers Finite Element Center
Chalmers University of Technology
SE–412 96 Göteborg Sweden
Göteborg, December 2001

A P^2-continuous, P^1-discontinuous finite element method for the Mindlin-Reissner plate model
Peter Hansbo and Mats G. Larson
NO 2001–22
ISSN 1404–4382

Chalmers Finite Element Center
Chalmers University of Technology
SE–412 96 Göteborg
Sweden
Telephone: +46 (0)31 772 1000
Fax: +46 (0)31 772 3595
`www.phi.chalmers.se`

Printed in Sweden
Chalmers University of Technology
Göteborg, Sweden 2001

A P^2-CONTINUOUS, P^1-DISCONTINUOUS FINITE ELEMENT METHOD FOR THE MINDLIN-REISSNER PLATE MODEL

PETER HANSBO AND MATS G. LARSON

ABSTRACT. We present a discontinuous finite element method for the Mindlin-Reissner plate model based on continuous piecewise second degree polynomials for the transverse displacements and discontinuous piecewise linear approximations for the rotations. We prove convergence, uniformly in the thickness of the plate, and thus show that locking is avoided. Finally, we present some numerical results.

1. Introduction

The differential equations describing the Mindlin-Reissner plate model can be derived from minimization of the sum of the bending energy, the shear energy, and the potential of the surface load,

$$\mathfrak{F}(u,\boldsymbol{\theta}) := \frac{1}{2}a(\boldsymbol{\theta},\boldsymbol{\theta}) + \frac{\kappa}{2\,t^2}\int_\Omega |\nabla u - \boldsymbol{\theta}|^2\, d\Omega - \int_\Omega g\, u\, d\Omega. \tag{1.1}$$

Here u is the transverse displacement, $\boldsymbol{\theta}$ is the rotation of the median surface, t is the thickness, $t^3\, g$ is the transverse surface load, and the bending energy $a(\cdot,\cdot)$ is defined by

$$a(\boldsymbol{\theta},\boldsymbol{\vartheta}) := \int_\Omega \Big(2\mu\boldsymbol{\varepsilon}(\boldsymbol{\theta}) : \boldsymbol{\varepsilon}(\boldsymbol{\vartheta}) + \lambda\nabla\cdot\boldsymbol{\theta}\,\nabla\cdot\boldsymbol{\vartheta}\Big)\, d\Omega,$$

where $\boldsymbol{\varepsilon}$ is the strain tensor. The material constants are given by the relations $\kappa = E\,k/(2(1+\nu))$, $\mu := E/(6(1+\nu))$, and $\lambda := \nu E/(12(1-\nu^2))$, where E and ν are the Young's modulus and Poisson's ratio, respectively, and $k \approx 5/6$ is a shear correction factor. We shall alternatively write the bending energy product as

$$a(\boldsymbol{\theta},\boldsymbol{\vartheta}) := \int_\Omega \boldsymbol{\sigma}(\boldsymbol{\theta}) : \boldsymbol{\varepsilon}(\boldsymbol{\vartheta})\, d\Omega,$$

where $\boldsymbol{\sigma}(\boldsymbol{\theta}) := 2\mu\boldsymbol{\varepsilon}(\boldsymbol{\theta}) + \lambda\nabla\cdot\boldsymbol{\theta}\,\mathbf{1}$ is the stress tensor.

The difficulty with this model, from a numerical point of view, is the matching of the approximating spaces for $\boldsymbol{\theta}$ and u. As $t \to 0$, the difference $\nabla u - \boldsymbol{\theta}$ must tend to zero, which, for naive choices of spaces, leads to a deterioration of the approximation known as

Date: December 20, 2001.

Key words and phrases. Mindlin–Reissner, discontinuous Galerkin, Nitsche's method, plate problem.

Peter Hansbo, Department of Applied Mechanics, Chalmers University of Technology, S–412 96 Göteborg, Sweden, *email*: hansbo@am.chalmers.se

Mats G. Larson, Department of Mathematics, Chalmers University of Technology, S–412 96 Göteborg, Sweden, *email*: mgl@math.chalmers.se.

locking. The situation is particularly difficult if we wish to use low order approximations. One useful approach has been to use projections in the shear energy term and consider modified energy functionals of the type

$$\mathfrak{F}_h(u,\boldsymbol{\theta}) := \frac{1}{2}a(\boldsymbol{\theta},\boldsymbol{\theta}) + \frac{\kappa}{2\,t^2}\int_\Omega |\nabla u - \boldsymbol{R}_h\boldsymbol{\theta}|^2\,d\Omega - \int_\Omega g\,u\,d\Omega, \tag{1.2}$$

where $\boldsymbol{R}_h$ is some interpolation or projection operator. This idea underpins, e.g., the MITC element family of Bathe and co-workers, first introduced in [2], and has been used extensively in the mathematical literature to prove convergence, see, e.g., [1, 4, 6, 11]. It should be noted that if the approximation corresponding to $\boldsymbol{R}_h\boldsymbol{\theta}$ were to be used also for the bending energy, the element would be non-conforming, and potentially unstable. This means that we in effect have to construct and match three different finite element spaces, and this is indeed how the approach was originally conceived: as a mixed method with an auxiliary set of unknowns (the shear stresses), cf. [2].

In this paper, we instead consider the use of a discontinuous Galerkin method based on discontinuous piecewise linear polynomials for the discretization of the rotations, in combination with continuous piecewise quadratic polynomials for the transverse displacements. Using this approach, there is no need for an independent approximation (or projection) of the shear stress term. The method can also be directly extended to higher order polynomials.

When the thickness of the plate tends to zero we obtain the Kirchoff plate and our scheme simplifies to the method proposed in [7]. In this context we also mention the recent discontinuous Galerkin method for the Kirchoff plate developed in [9].

2. The finite element method

For simplicity, we shall assume that the domain Ω is a convex polygon and consider the case of clamped boundary conditions. The transverse displacement and rotation vector are solutions to the following variational problem: find $\boldsymbol{\theta} \in [H^1_0(\Omega)]^2$ and $u \in H^1_0(\Omega)$ such that

$$\int_\Omega \boldsymbol{\sigma}(\boldsymbol{\theta}) : \boldsymbol{\varepsilon}(\boldsymbol{\vartheta})\,d\Omega + \frac{\kappa}{t^2}\int_\Omega (\nabla u - \boldsymbol{\theta})\cdot(\nabla v - \boldsymbol{\vartheta})\;d\Omega = \int_\Omega g\,v\,d\Omega \tag{2.1}$$

for all $(v,\boldsymbol{\vartheta}) \in H^1_0(\Omega)\times[H^1_0(\Omega)]^2$.

To define the method, consider a subdivision $\mathcal{T} = \{T\}$ of Ω into a geometrically conforming, quasiuniform, finite element mesh. Denote by h_T the diameter of element T and by $h = \max_{T\in\mathcal{T}} h_T$ the global mesh size parameter. We shall use continuous, piecewise polynomial, approximations of the transverse displacement:

$$V_h = \{v \in H^1_0(\Omega)\cap C^0(\Omega) :\ v|_T \in P^2(T) \text{ for all } T\in\mathcal{T}\}.$$

Further, for the approximation of the rotations, we will use the following finite element space:

$$\boldsymbol{\Theta}_h := \{\boldsymbol{\vartheta} \in [L^2(\Omega)]^2 :\ \boldsymbol{\vartheta}|_T \in [P^1(T)]^2 \text{ for all } T\in\mathcal{T}\},$$

i.e., the space of piecewise linear, discontinuous, functions.

The point of these choices is the inclusion

$$\nabla V_h \subset \boldsymbol{\Theta}_h \tag{2.2}$$

so that, in the limit $t \to 0$, functions in $\boldsymbol{\Theta}_h$ are allowed to belong to ∇V_h which retains enough approximation power to allow optimal order convergence.

To define our method we introduce the set of edges in the mesh, $\mathcal{E} = \{E\}$, and we split $\mathcal{E}$ into two disjoint subsets

$$\mathcal{E} = \mathcal{E}_I \cup \mathcal{E}_B,$$

where $\mathcal{E}_I$ is the set of edges in the interior of Ω and $\mathcal{E}_B$ is the set of edges on the boundary. Further, with each edge we associate a fixed unit normal $\boldsymbol{n}$ such that for edges on the boundary $\boldsymbol{n}$ is the exterior unit normal. We denote the jump of a function $\boldsymbol{v} \in \boldsymbol{\Gamma}_h$ at an edge E by $[\boldsymbol{v}] = \boldsymbol{v}^+ - \boldsymbol{v}^-$ for $E \in \mathcal{E}_I$ and $[\boldsymbol{v}] = \boldsymbol{v}^+$ for $E \in \mathcal{E}_B$, and the average $\langle \boldsymbol{v} \rangle = (\boldsymbol{v}^+ + \boldsymbol{v}^-)/2$ for $E \in \mathcal{E}_I$ and $\langle \boldsymbol{v} \rangle = \boldsymbol{v}^+$ for $E \in \mathcal{E}_B$, where $\boldsymbol{v}^\pm = \lim_{\epsilon \downarrow 0} \boldsymbol{v}(\boldsymbol{x} \mp \epsilon\, \boldsymbol{n})$ with $\boldsymbol{x} \in E$.

Our method can now be formulated as follows: find $\boldsymbol{\theta}^h \in \boldsymbol{\Theta}_h$ and $u^h \in V_h$ such that

$$a_h(\boldsymbol{\theta}^h, \boldsymbol{\vartheta}) + \frac{\kappa}{t^2}\left(\nabla u^h - \boldsymbol{\theta}^h, \nabla v - \boldsymbol{\vartheta}\right) = (g, v) \tag{2.3}$$

for all $(v, \boldsymbol{\vartheta}) \in V_h \times \boldsymbol{\Theta}_h$. In (2.3), $(\cdot,\cdot)$ denotes the usual L_2 scalar product and the bilinear form $a_h(\cdot,\cdot)$ is defined by

$$\begin{aligned} a_h(\boldsymbol{\theta}^h, \boldsymbol{\vartheta}) \;&= \sum_{T\in\mathcal{T}} \int_T \boldsymbol{\sigma}(\boldsymbol{\theta}^h) : \boldsymbol{\varepsilon}(\boldsymbol{\vartheta})\, dxdy \\ &- \sum_{E\in\mathcal{E}_I\cup\mathcal{E}_B} \int_E \left(\langle \boldsymbol{n}\cdot\boldsymbol{\sigma}(\boldsymbol{\theta}^h)\rangle \cdot [\boldsymbol{\vartheta}] + \langle \boldsymbol{n}\cdot\boldsymbol{\sigma}(\boldsymbol{\vartheta})\rangle \cdot [\boldsymbol{\theta}^h]\right)\, ds \\ &+ (2\mu + 3\lambda)\,\gamma \sum_{E\in\mathcal{E}_I\cup\mathcal{E}_B} \int_E h_E^{-1} [\boldsymbol{\theta}^h] \cdot [\boldsymbol{\vartheta}]\; ds. \end{aligned}$$

Here γ is a positive constant and h_E is defined by

$$h_E = \left(|T^+| + |T^-|\right)/(2\,|E|) \quad \text{for } E = \partial T^+ \cap \partial T^-, \tag{2.4}$$

with $|T|$ the area of T, on each edge.

Using Green's formula, we readily establish the following Lemma.

Lemma 2.1. *The method* (2.3) *is consistent in the sense that*

$$a_h(\boldsymbol{\theta} - \boldsymbol{\theta}^h, \boldsymbol{\vartheta}) + \frac{\kappa}{t^2}\left(\nabla u - \nabla u^h - (\boldsymbol{\theta} - \boldsymbol{\theta}^h), \nabla v - \boldsymbol{\vartheta}\right) = 0$$

for all $\boldsymbol{\vartheta} \in \boldsymbol{\Theta}_h$ *and* $v \in V_h$*.*

3. Stability estimates

For our analysis, we introduce the following mesh dependent energy norm

$$|||\boldsymbol{\vartheta}|||^2 = \sum_{T\in\mathcal{T}} \int_T \boldsymbol{\sigma}(\boldsymbol{\vartheta}) : \boldsymbol{\varepsilon}(\boldsymbol{\vartheta})\, dxdy + (2\mu + 3\lambda) \sum_{E\in\mathcal{E}_I\cup\mathcal{E}_B} \int_E h_E^{-1}\, [\boldsymbol{\vartheta}] \cdot [\boldsymbol{\vartheta}]\; ds, \tag{3.1}$$

and the edge norm

$$\|\boldsymbol{\vartheta}\|^2 = \sum_{E\in\mathcal{E}_I\cup\mathcal{E}_B} \|\boldsymbol{\vartheta}\|^2_{L^2(E)}. \tag{3.2}$$

The mesh dependent norm $|||\cdot|||$ can be used to bound the broken $H^1(\Omega)$ norm on $\boldsymbol{\Theta}_h$, which is the statement of the following Lemma.

Lemma 3.1. *There is a constant c, independent of h, μ, and λ such that*

$$\sum_{T\in\mathcal{T}} \|\boldsymbol{\vartheta}\|^2_{H^1(T)} \leq c|||\boldsymbol{\vartheta}|||^2 \quad \textit{for all } \boldsymbol{\vartheta}\in\boldsymbol{\Theta}_h. \tag{3.3}$$

Proof. This is a discrete Korn-type inequality that results from the control of the rigid body rotations given by the jump terms. A complete proof can be found in [8]. □

In order to show that the method (2.3) is stable, we shall first show that $a_h(\cdot,\cdot)$ is coercive with respect to the norm $|||\cdot|||$, given that γ is sufficiently large.

Lemma 3.2. *If $\gamma_{>}c_0$, with c_0 sufficiently large, then the following estimate holds*

$$c\,|||\boldsymbol{\vartheta}|||^2 \leq a_h(\boldsymbol{\vartheta},\boldsymbol{\vartheta}), \tag{3.4}$$

for all $\boldsymbol{v}\in\boldsymbol{\Theta}_h$.

Proof. We first note that the following inverse estimate holds

$$\|h^{1/2}\langle\boldsymbol{n}\cdot\boldsymbol{\sigma}(\boldsymbol{\vartheta})\rangle\|^2_{\mathcal{E}_I\cup\mathcal{E}_B} \leq c_I \sum_{T\in\mathcal{T}} \|\boldsymbol{\sigma}(\boldsymbol{\vartheta})\|^2_T. \tag{3.5}$$

This inequality is proved by scaling and finite dimensionality (see, e.g. [12]). Next we note that

$$\frac{1}{2\mu+3\lambda}\|\boldsymbol{\sigma}(\boldsymbol{\vartheta})\|^2_T \leq (\boldsymbol{\sigma}(\boldsymbol{\vartheta}),\boldsymbol{\varepsilon}(\boldsymbol{\vartheta}))_T,$$

cf. [8], and thus we conclude that

$$\frac{1}{2\mu+3\lambda}\|h^{1/2}\langle\boldsymbol{n}\cdot\boldsymbol{\sigma}(\boldsymbol{\vartheta})\rangle\|^2_{\mathcal{E}_I\cup\mathcal{E}_B} \leq c_I \sum_{T\in\mathcal{T}} (\boldsymbol{\sigma}(\boldsymbol{\vartheta}),\boldsymbol{\varepsilon}(\boldsymbol{\vartheta}))_T. \tag{3.6}$$

Next, we have, for each $E\in\mathcal{E}_I\cup\mathcal{E}_B$, that

$$\begin{aligned} 2(\langle\boldsymbol{n}\cdot\boldsymbol{\sigma}(\boldsymbol{\vartheta})\rangle\,,[\boldsymbol{\vartheta}])_E &= 2(\langle\boldsymbol{n}\cdot\boldsymbol{\sigma}(\boldsymbol{\vartheta})\rangle\,,[\boldsymbol{\vartheta}])_E \\ &\leq \delta(2\mu+3\lambda)^{-1}\|h^{1/2}\,\langle\boldsymbol{n}\cdot\boldsymbol{\sigma}(\boldsymbol{\vartheta})\rangle\,\|^2_E \\ &\qquad +\delta^{-1}(2\mu+3\lambda)\|h^{-1/2}[\boldsymbol{\vartheta}]\|^2_E, \end{aligned}$$

where we used the Cauchy-Schwarz inequality followed by the arithmetic-geometric mean inequality. Using these estimates and choosing δ small enough, we obtain

$$\begin{aligned} a_h(\boldsymbol{\vartheta},\boldsymbol{\vartheta}) &\geq (1-c_I\delta)\sum_{T\in\mathcal{T}}(\boldsymbol{\sigma}(\boldsymbol{\vartheta}),\boldsymbol{\varepsilon}(\boldsymbol{\vartheta}))_T + (2\mu+3\lambda)(\gamma-\delta^{-1})\|h^{-1/2}[\boldsymbol{\vartheta}]\|^2_{\mathcal{E}_I\cup\mathcal{E}_B} \\ &\geq c|||\boldsymbol{\vartheta}|||^2, \end{aligned}$$

whence we must choose $\gamma\geq c_0 > c_I$. □

We have thus shown the following stability property of the method.

Proposition 3.3. *Choosing $\gamma \geq c_0 > c_I$, the following coercivity condition holds:*

$$a_h(\boldsymbol{\vartheta}, \boldsymbol{\vartheta}) + \frac{\kappa}{t^2} \int_\Omega |\nabla v - \boldsymbol{\vartheta}|^2 d\Omega \geq C\Big(|||\boldsymbol{\vartheta}||| + \kappa^{1/2} t^{-1} \|\nabla v - \boldsymbol{\vartheta}\|_{L_2(\Omega)} \Big)^2, \tag{3.7}$$

for all $(\boldsymbol{\vartheta}, v) \in \boldsymbol{\Theta}_h \times V_h$.

We finally remark that the constant c_I in the inverse estimate (3.5) is computable and thus the lower bound c_0 on γ is available, see [10] for details.

4. Error estimates

For convenience, we introduce the scaled shear stress $\boldsymbol{\zeta}$ and its discrete counterpart $\boldsymbol{\zeta}^h$, defined by

$$\boldsymbol{\zeta} := \kappa^{1/2}(\nabla u - \boldsymbol{\theta})/t^2 \quad \text{and} \quad \boldsymbol{\zeta}^h := \kappa^{1/2}(\nabla u^h - \boldsymbol{\theta}^h)/t^2. \tag{4.1}$$

We also split the Mindlin-Reissner displacement u into the corresponding Kirchhoff solution u_0 corresponding to the limit case $t \to 0$, and a remainder u_r, so that $u = u_0 + u_r$. We then have the following stability estimate.

Lemma 4.1. *Assume that Ω is convex and $g \in L_2(\Omega)$. Then*

$$\|u_0\|_{H^3(\Omega)} + \frac{1}{t}\|u_r\|_{H^2(\Omega)} + \|\theta\|_{H^2(\Omega)} + t\|\boldsymbol{\zeta}\|_{H^1(\Omega)} \leq C\Big(\|g\|_{H^{-1}(\Omega)} + t\|g\|_{L_2(\Omega)} \Big).$$

For a proof, see Chapelle and Stenberg [5].

For the purpose of analysis, we introduce the nodal interpolation operators $\boldsymbol{\pi}_1 : [H^2(\Omega)]^2 \to \boldsymbol{W}_h$, where

$$\boldsymbol{W}_h := \{\boldsymbol{v} \in [H^1(\Omega) \cap C^0(\Omega)]^2 : \ \boldsymbol{v}|_T \in [P^1(T)]^2 \text{ for all } T \in \mathcal{T}\},$$

and $\pi_2 : H^2(\Omega) \to V_h$. We also define the operators $\boldsymbol{P}_u : [H^2(\Omega)]^2 \to \boldsymbol{\Theta}_h$ and $\boldsymbol{Q}_u : [H^2(\Omega)]^2 \to \boldsymbol{\Theta}_h$ defined by

$$\boldsymbol{P}_u \boldsymbol{\theta} := \nabla \pi_2 u_0 - \boldsymbol{\pi}_1 \nabla u_0 + \boldsymbol{\pi}_1 \boldsymbol{\theta}$$

and

$$\boldsymbol{Q}_u \boldsymbol{\zeta} := \kappa^{1/2} \left(\nabla \pi_2 u_r - \boldsymbol{\pi}_1 \nabla u_r)\right)/t^2 + \boldsymbol{\pi}_1 \boldsymbol{\zeta}.$$

Noting that

$$\frac{t^2}{\kappa^{1/2}} \boldsymbol{Q}_u \boldsymbol{\zeta} = \nabla \pi_2 u_r - \boldsymbol{\pi}_1 \nabla u_r + \boldsymbol{\pi}_1 \nabla (u_r + u_0) + \boldsymbol{\pi}_1 \boldsymbol{\theta} = \nabla \pi_2 u - \boldsymbol{P}_u \boldsymbol{\theta},$$

and using Lemma 2.1, we then find

$$a_h(\boldsymbol{\theta} - \boldsymbol{\theta}^h, \boldsymbol{P}_u \boldsymbol{\theta}) + t^2(\boldsymbol{\zeta} - \boldsymbol{\zeta}^h, \boldsymbol{Q}_u \boldsymbol{\zeta}) = 0. \tag{4.2}$$

We will need the following approximation properties of our finite element subspaces.

Lemma 4.2. *We have the following interpolation estimate:*

$$
\begin{aligned}
(4.3) \qquad & |||\boldsymbol{\theta} - \boldsymbol{P}_u\boldsymbol{\theta}||| + t\|\boldsymbol{\zeta} - \boldsymbol{Q}_u\boldsymbol{\zeta}\|_{L_2(\Omega)} \\
& \qquad \leq Ch\Big(\|\boldsymbol{\theta}\|_{H^2(\Omega)} + \|u_0\|_{H^3(\Omega)} + t^{-1}\|u_r\|_{H^2(\Omega)} + \|\boldsymbol{\zeta}\|_{H^1(\Omega)}\Big).
\end{aligned}
$$

Proof. We first recall the trace inequality (cf. [12])

$$
h_T^{-1}\|\boldsymbol{\vartheta}\|^2_{L_2(\partial T)} \leq C\left(h_T^{-2}\|\boldsymbol{\vartheta}\|^2_{L_2(T)} + \|\boldsymbol{\vartheta}\|^2_{H^1(T)}\right), \quad \forall \boldsymbol{\vartheta} \in [H^2(T)]^2. \tag{4.4}
$$

For the edge norm we have that

$$
h_E^{-1}\|[\boldsymbol{\theta} - \boldsymbol{P}_u\boldsymbol{\theta}]\|^2_{L_2(E)} \leq Ch_E^{-1}\Big(\|\boldsymbol{\theta} - \boldsymbol{P}_u\boldsymbol{\theta}\|^2_{L_2(\partial T_1)} + \|\boldsymbol{\theta} - \boldsymbol{P}_u\boldsymbol{\theta}\|^2_{L_2(\partial T_2)}\Big)
$$

for E shared by adjacent elements T_1 and T_2, and since, by quasiuniformity, $h_{T_i} \leq h_E/C$, $i = 1, 2$, we find, using (4.4),

$$
\begin{aligned}
h_E^{-1}\|\boldsymbol{\theta} - \boldsymbol{P}_u\boldsymbol{\theta}\|^2_{L_2(\partial T_i)} &\leq Ch_{T_i}^{-1}\|\boldsymbol{\theta} - \boldsymbol{P}_u\boldsymbol{\theta}\|^2_{L_2(\partial T_i)} \\
&\leq C\left(h_{T_i}^{-2}\|\boldsymbol{\theta} - \boldsymbol{P}_u\boldsymbol{\theta}\|^2_{L_2(T_i)} + \|\boldsymbol{\theta} - \boldsymbol{P}_u\boldsymbol{\theta}\|^2_{H^1(T_i)}\right).
\end{aligned}
$$

Using the definition of $\boldsymbol{P}_u$ and applying the triangle inequality, we find

$$
\|\boldsymbol{\theta} - \boldsymbol{P}_u\boldsymbol{\theta}\| \leq \|\boldsymbol{\theta} - \boldsymbol{\pi}_1\boldsymbol{\theta}\| + \|\nabla u_0 - \nabla\pi_2 u_0\| + \|\nabla u_0 - \boldsymbol{\pi}_1\nabla u_0\|,
$$

so that, by standard interpolation theory,

$$
h_E^{-1}\|\boldsymbol{\theta} - \boldsymbol{P}_u\boldsymbol{\theta}\|^2_{L_2(\partial T_i)} \leq Ch_T^2\Big(\|\boldsymbol{\theta}\|^2_{H^2(T_i)} + \|u_0\|^2_{H^3(T_i)}\Big).
$$

Similarly,

$$
\int_T \boldsymbol{\sigma}(\boldsymbol{\theta} - \boldsymbol{P}_u\boldsymbol{\theta}) : \boldsymbol{\varepsilon}(\boldsymbol{\theta} - \boldsymbol{P}_u\boldsymbol{\theta})\, dxdy \leq Ch_T^2\Big(\|\boldsymbol{\theta}\|^2_{H^2(T)} + \|u_0\|^2_{H^3(T)}\Big).
$$

By summation it thus follows that

$$
|||\boldsymbol{\theta} - \boldsymbol{\pi}_u\boldsymbol{\theta}||| \leq Ch\Big(\|\boldsymbol{\theta}\|_{H^2(\Omega)} + \|u_0\|_{H^3(\Omega)}\Big).
$$

Finally, by the triangle inequality and standard interpolation arguments,

$$
\begin{aligned}
\|\boldsymbol{\zeta} - \boldsymbol{Q}_u\boldsymbol{\zeta}\|_{L_2(\Omega)} &\leq \|\boldsymbol{\zeta} - \boldsymbol{\pi}_1\boldsymbol{\zeta}\|_{L_2(\Omega)} + \frac{\kappa^{1/2}}{t^2}\|\nabla u_r - \nabla\pi_2 u_r\|_{L_2(\Omega)} \\
&\qquad + \frac{\kappa^{1/2}}{t^2}\|\nabla u_r - \boldsymbol{\pi}_1\nabla u_r\|_{L_2(\Omega)} \\
&\leq Ch\Big(t^{-2}\|u_r\|_{H^2(\Omega)} + \|\boldsymbol{\zeta}\|_{H^1(\Omega)}\Big),
\end{aligned}
$$

which completes the proof of the lemma. □

We can now prove the following best approximation result.

Lemma 4.3. *We have that*

$$
|||\boldsymbol{\theta} - \boldsymbol{\theta}^h||| + t\|\boldsymbol{\zeta} - \boldsymbol{\zeta}^h\|_{L_2(\Omega)} \leq C\Big(|||\boldsymbol{\theta} - \boldsymbol{P}_u\boldsymbol{\theta}||| + t\|\boldsymbol{\zeta} - \boldsymbol{Q}_u\boldsymbol{\zeta}\|_{L_2(\Omega)}\Big).
$$

Proof. By the triangle inequality

$$|||\boldsymbol{\theta}-\boldsymbol{\theta}^h||| + t\|\boldsymbol{\zeta}-\boldsymbol{\zeta}^h\|_{L_2(\Omega)} \le |||\boldsymbol{\theta}-\boldsymbol{P}_u\boldsymbol{\theta}||| + |||\boldsymbol{P}_u\boldsymbol{\theta}-\boldsymbol{\theta}^h||| \\ + t\Big(\|\boldsymbol{\zeta}-\boldsymbol{Q}_u\boldsymbol{\zeta}\|_{L_2(\Omega)} + \|\boldsymbol{Q}_u\boldsymbol{\zeta}-\boldsymbol{\zeta}^h\|_{L_2(\Omega)}\Big).$$

Further, by (4.2), we have that

$$\begin{aligned} &|||\boldsymbol{\theta}^h-\boldsymbol{P}_u\boldsymbol{\theta}|||^2 + t^2\|\boldsymbol{\zeta}^h-\boldsymbol{Q}_u\boldsymbol{\zeta}\|^2_{L_2(\Omega)} \\ &\quad\le Ca_h(\boldsymbol{\theta}^h-\boldsymbol{P}_u\boldsymbol{\theta},\boldsymbol{\theta}^h-\boldsymbol{P}_u\boldsymbol{\theta}) + t^2(\boldsymbol{\zeta}^h-\boldsymbol{Q}_u\boldsymbol{\zeta},\boldsymbol{\zeta}^h-\boldsymbol{Q}_u\boldsymbol{\zeta}) \\ &\quad= Ca_h(\boldsymbol{\theta}-\boldsymbol{P}_u\boldsymbol{\theta},\boldsymbol{\theta}^h-\boldsymbol{P}_u\boldsymbol{\theta}) + t^2(\boldsymbol{\zeta}-\boldsymbol{Q}_u\boldsymbol{\zeta},\boldsymbol{\zeta}^h-\boldsymbol{Q}_u\boldsymbol{\zeta}) \\ &\quad\le C\Big(|||\boldsymbol{\theta}-\boldsymbol{P}_u\boldsymbol{\theta}||| + t\|\boldsymbol{\zeta}-\boldsymbol{Q}_u\boldsymbol{\zeta}\|_{L_2(\Omega)}\Big)\Big(|||\boldsymbol{\theta}^h-\boldsymbol{P}_u\boldsymbol{\theta}||| + t\|\boldsymbol{\zeta}^h-\boldsymbol{Q}_u\boldsymbol{\zeta}\|_{L_2(\Omega)}\Big), \end{aligned}$$

and the lemma follows. □

Finally, combining Lemmas 4.1, 4.2, and 4.3, we obtain

Theorem 4.4. *If Ω is a convex domain and $g \in L_2(\Omega)$ we have, for $(\boldsymbol{\theta}^h, u^h)$ solving* (2.3) *and $(\boldsymbol{\theta}, u)$ solving* (2.1)*, and using the definition* (4.1)*,*

$$|||\boldsymbol{\theta}-\boldsymbol{\theta}^h||| + t\|\boldsymbol{\zeta}-\boldsymbol{\zeta}^h\|_{L_2(\Omega)} \le Ch\Big(\|g\|_{H^{-1}(\Omega)} + t\|g\|_{L_2(\Omega)}\Big),$$

uniformly in t.

5. Numerical examples

5.1. **Locking.** In order to solve a problem with known exact solution, we consider a Kirchhoff solution

$$u = (1-x)^2\, x^2\, (1-y)^2\, y^2,$$

and compute the corresponding load on the domain $\Omega = (0,1)\times(0,1)$. The material parameters and thickness are $E = 10^9$, $\nu = 1/2$, and $t = 10^{-6}$. With such a small thickness, the Mindlin-Reissner solution will be so close to the Kirchhoff solution that the latter can be used for convergence studies. The imposed boundary conditions are accordingly set to $u = 0$, $\boldsymbol{\theta} = 0$ on $\partial\Omega$.

We show the effect of the parameter γ from (2.4). It is clear that γ cannot be chosen too large in general, since this will prevent $\boldsymbol{\theta}$ from approximating ∇u as $t \to 0$. In Figure 1, we show how the ratio between the approximate solution and the exact solution at the midpoint is affected by the meshize and by γ. It is seen that on coarse meshes, an increased γ tends to lock the solution.

5.2. **Convergence.** We show, for the same example as previously, the convergence in $H^1(\Omega)$. The difference between ∇u^h and $\boldsymbol{\theta}^h$ is so small for this choice of thickness that we can equate this norm with $a_h(\boldsymbol{\theta}-\boldsymbol{\theta}^h,\boldsymbol{\theta}-\boldsymbol{\theta}^h)^{1/2}$. As can be seen from Figure 2, we in fact obtain slighter better than first order convergence.

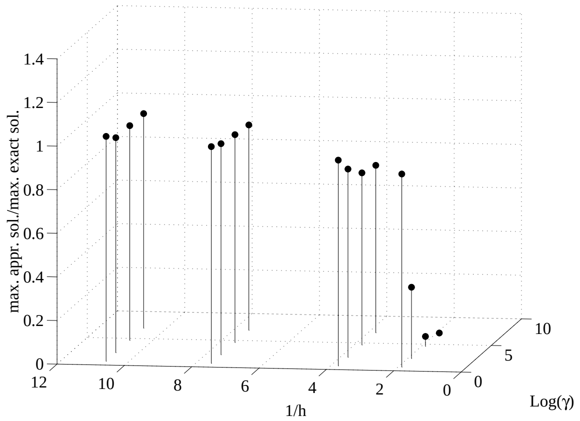

FIGURE 1. Locking for large γ:s.

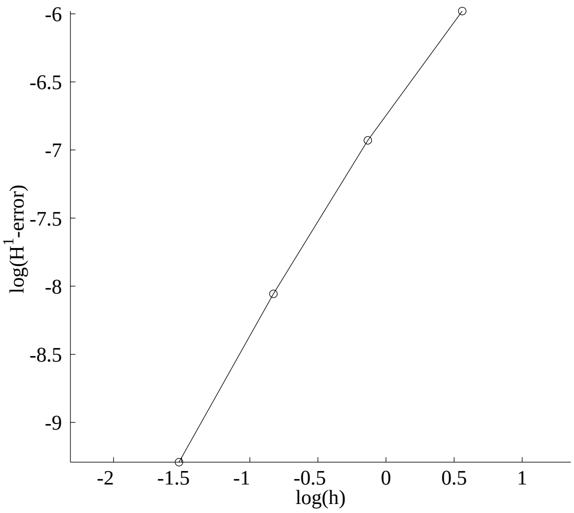

FIGURE 2. Convergence of u^h in $H^1(\Omega)$.

6. Concluding remarks

We have presented a novel finite element method for the Mindlin-Reissner plate model, based on the discontinuous Galerkin approach. We show that our method does not lock as long as we make a proper choice of a free, but computable, parameter. Our approach avoids the current paradigm of projections of the rotations in the shear energy functional, which, at least from a conceptual point of view, requires a mixed implementation. We pay the prize of having to use a higher number of degrees of freedom; in consequence, the presented approach may not be computationally competitive with the "best" elements available. Nevertheless, we feel that it is a very simple and straightforward method; in particular it is free of special mixed element approximations.

References

[1] Arnold, D. N. and Falk, R. S. (1989) A uniformly accurate finite-element method for the Reissner-Mindlin plate. SIAM J. Numer. Anal. **26**, 1276–1290

[2] Bathe, K. J. and Dvorkin, E. N. (1985) A four-node plate bending element based on Mindlin-Reissner plate theory and mixed interpolation. Int. J. Numer. Methods Engrg. **21**, 367–383

[3] Brezzi, F. and Fortin, M. (1991) Mixed and Hybrid Finite Element Methods. Springer, New York

[4] Brezzi, F., Fortin, M., and Stenberg, R. (1991) Error analysis of mixed-interpolated elements for Reissner–Mindlin plates. Math. Models Methods Appl. Sci. **1**, 125–151

[5] Chapelle, D. and Stenberg, R. (1998) An optimal low-order locking-free finite element method for Reissner-Mindlin plates. Math. Models Methods Appl. Sci. **8**, 407–430

[6] Duran, R. and Liberman, E. (1992) On mixed finite-element methods for the Reissner-Mindlin plate model. Math. Comput., **58**, 561–573

[7] Engel, G., Garikipati, K., Hughes, T. J. R., Larson, M. G., Mazzei, L., and Taylor, R. L. (2001) Continuous/discontinuous approximations of fourth-order elliptic problems in structural and continuum mechanics with applications to thin bending elements and strain gradient elasticity, submitted to Comput. Methods Appl. Mech. Engrg.

[8] Hansbo, P. and Larson, M. G. (2000) Discontinuous Galerkin and the Crouzeix-Raviart element: Application to elasticity, Chalmers Finite Element Center Preprint 2000-09, Chalmers University of Technology, Sweden

[9] Hansbo, P. and Larson, M. G. (2000) A discontinuous Galerkin method for the plate problem, Chalmers Finite Element Center Preprint 2000-08, Chalmers University of Technology, Sweden, to appear in Calcolo.

[10] Hansbo, P. and Larson, M. G. (2000) Discontinuous Galerkin methods for nearly incompressible elasticity by Nitsche's method, Chalmers Finite Element Center Preprint 2000-06, Chalmers University of Technology, Sweden, to appear in Comput. Methods Appl. Mech. Engrg.

[11] Pitkäranta, J. (1988) Analysis of some low-order finite-element schemes for Mindlin-Reissner and Kirchhoff plates. Numer. Math. **53**, 237–254

[12] Thomée, V. (1997) Galerkin Finite Element Methods for Parabolic Problems. Springer-Verlag, Berlin

Chalmers Finite Element Center Preprints

2000–01 *Adaptive finite element methods for the unsteady Maxwell's equations*
Johan Hoffman

2000–02 *A multi-adaptive ODE-solver*
Anders Logg

2000–03 *Multi-adaptive error control for ODEs*
Anders Logg

2000–04 *Dynamic computational subgrid modeling* (Licentiate Thesis)
Johan Hoffman

2000–05 *Least-squares finite element methods for electromagnetic applications* (Licentiate Thesis)
Rickard Bergström

2000–06 *Discontinuous galerkin methods for incompressible and nearly incompressible elasticity by Nitsche's method*
Peter Hansbo and Mats G. Larson

2000–07 *A discountinuous Galerkin method for the plate equation*
Peter Hansbo and Mats G. Larson

2000–08 *Conservation properties for the continuous and discontinuous Galerkin methods*
Mats G. Larson and A. Jonas Niklasson

2000–09 *Discontinuous Galerkin and the Crouzeix-Raviart element: application to elasticity*
Peter Hansbo and Mats G. Larson

2000–10 *Pointwise a posteriori error analysis for an adaptive penalty finite element method for the obstacle problem*
Donald A. French, Stig Larson and Ricardo H. Nochetto

2000–11 *Global and localised a posteriori error analysis in the maximum norm for finite element approximations of a convection-diffusion Problem*
Mats Boman

2000–12 *A posteriori error analysis in the maximum norm for a penalty finite element method for the time-dependent obstacle problem*
Mats Boman

2000–13 *A posteriori error analysis in the maximum norm for finite element approximations of a time-dependent convection-diffusion problem*
Mats Boman

2001–01 *A simple nonconforming bilinear element for the elasticity problem*
Peter Hansbo and Mats G. Larson

2001–02 *The $\mathcal{LL}^*$ finite element method and multigrid for the magnetostatic problem*
Rickard Bergström, Mats G. Larson, and Klas Samuelsson

2001–03 *The Fokker-Planck operator as an asymptotic limit in anisotropic media*
Mohammad Asadzadeh

2001–04 *A posteriori error estimation of functionals in elliptic problems: experiments*
Mats G. Larson and A. Jonas Niklasson

2001–05 *A note on energy conservation for Hamiltonian systems using continuous time finite elements*
Peter Hansbo

2001–06 *Stationary level set method for modelling sharp interfaces in groundwater flow*
Nahidh Sharif and Nils-Erik Wiberg

2001–07 *Integration methods for the calculation of the magnetostatic field due to coils*
Marzia Fontana

2001–08 *Adaptive finite element computation of 3D magnetostatic problems in potential formulation*
Marzia Fontana

2001–09 *Multi-adaptive galerkin methods for ODEs I: theory & algorithms*
Anders Logg

2001–10 *Multi-adaptive galerkin methods for ODEs II: applications*
Anders Logg

2001–11 *Energy norm a posteriori error estimation for discontinuous Galerkin methods*
Roland Becker, Peter Hansbo, and Mats G. Larson

2001–12 *Analysis of a family of discontinuous Galerkin methods for elliptic problems: the one dimensional case*
Mats G. Larson and A. Jonas Niklasson

2001–13 *Analysis of a nonsymmetric discontinuous Galerkin method for elliptic problems: stability and energy error estimates*
Mats G. Larson and A. Jonas Niklasson

2001–14 *A hybrid method for the wave equation*
Larisa Beilina, Klas Samuelsson and Krister Åhlander

2001–15 *A finite element method for domain decomposition with non-matching grids*
Roland Becker, Peter Hansbo and Rolf Stenberg

2001–16 *Application of stable FEM-FDTD hybrid to scattering problems*
Thomas Rylander and Anders Bondeson

2001–17 *Eddy current computations using adaptive grids and edge elements*
Y. Q. Liu, A. Bondeson, R. Bergström, C. Johnson, M. G. Larson, and K. Samuelsson

2001–18 *Adaptive finite element methods for incompressible fluid flow*
Johan Hoffman and Claes Johnson

2001–19 *Dynamic subgrid modeling for time dependent convection–diffusion–reaction equations with fractal solutions*
Johan Hoffman

2001–20 *Topics in adaptive computational methods for differential equations*
Claes Johnson, Johan Hoffman and Anders Logg

2001–21 *An unfitted finite element method for elliptic interface problems*
Anita Hansbo and Peter Hansbo

2001–22 *A P^2–continuous, P^1–discontinuous finite element method for the Mindlin-Reissner plate model*
Peter Hansbo and Mats G. Larson

These preprints can be obtained from

`www.phi.chalmers.se/preprints`